

# Characterization of Brca2-Deficient Plants Excludes the Role of NHEJ and SSA in the Meiotic Chromosomal Defect Phenotype

Marilyn Dumont, Sophie Massot, Marie-Pascale Doutriaux, Ariane Gratias\*

Institut de Biologie des Plantes, CNRS UMR8618, Université Paris Sud-11, Orsay, France

## Abstract

In somatic cells, three major pathways are involved in the repair of DNA double-strand breaks (DSB): Non-Homologous End Joining (NHEJ), Single-Strand Annealing (SSA) and Homologous Recombination (HR). In somatic and meiotic HR, DNA DSB are 5' to 3' resected, producing long 3' single-stranded DNA extensions. Brca2 is essential to load the Rad51 recombinase onto these 3' overhangs. The resulting nucleofilament can thus invade a homologous DNA sequence to copy and restore the original genetic information. In *Arabidopsis*, the inactivation of Brca2 specifically during meiosis by an RNAi approach results in aberrant chromosome aggregates, chromosomal fragmentation and missegregation leading to a sterility phenotype. We had previously suggested that such chromosomal behaviour could be due to NHEJ. In this study, we show that knock-out plants affected in both *BRCA2* genes show the same meiotic phenotype as the RNAi-inactivated plants. Moreover, it is demonstrated that during meiosis, neither NHEJ nor SSA compensate for HR deficiency in *BRCA2*-inactivated plants. The role of the plant-specific DNA Ligase6 is also excluded. The possible mechanism(s) involved in the formation of these aberrant chromosomal bridges in the absence of HR during meiosis are discussed.

**Citation:** Dumont M, Massot S, Doutriaux M-P, Gratias A (2011) Characterization of Brca2-Deficient Plants Excludes the Role of NHEJ and SSA in the Meiotic Chromosomal Defect Phenotype. PLoS ONE 6(10): e26696. doi:10.1371/journal.pone.0026696

**Editor:** Marco Muzi-Falconi, Università di Milano, Italy

**Received:** June 8, 2011; **Accepted:** October 2, 2011; **Published:** October 21, 2011

**Copyright:** © 2011 Dumont et al. This is an open-access article distributed under the terms of the Creative Commons Attribution License, which permits unrestricted use, distribution, and reproduction in any medium, provided the original author and source are credited.

**Funding:** This work was supported by the Centre National de la Recherche Scientifique and the Université Paris Sud-11. M.D. is the recipient of a French Ministère de L'Enseignement Supérieur et de la Recherche doctoral fellowship. The funders had no role in study design, data collection and analysis, decision to publish, or preparation of the manuscript.

**Competing Interests:** The authors have declared that no competing interests exist.

\* E-mail: ariane.gratias-weill@u-psud.fr

## Introduction

One of the most cytotoxic DNA damage is chromosomal breakage, where a DNA double-strand break (DSB) occurs in the duplex DNA. Failure to repair correctly even one DNA DSB can result in the loss of genetic information, chromosome rearrangement, mutations and lead eventually to cell death. In plants, as in other organisms, cells have developed powerful and rapid cellular responses, leading to cell cycle arrest and DNA DSB repair. In eukaryotes, DNA broken ends can be processed by three major DSB repair pathways that are tightly regulated, depending on cell type and cell cycle phase: Non-Homologous End Joining (NHEJ), Single-strand annealing (SSA), and Homologous Recombination (HR).

In the NHEJ pathway, DNA broken ends are simply joined with little or no further processing. In mammalian cells, the Ku70-Ku80 heterodimer forms a ternary complex with the DNA-PKcs, and binds to the DSB. The binding of this complex prevents excessive degradation and promotes the recruitment of other factors involved in the processing of DNA ends to make them suitable for the ultimate step of ligation by the LigaseIV-Xrcc4 complex [1,2]. While no ortholog of DNA-PKcs has been found in *Arabidopsis*, *AtKu70*, *AtKu80*, *AtLigIV* and *AtXrcc4* homologs have been identified [3,4,5,6]. Mammalian null mutants affected in the NHEJ pathway present various orders of phenotype severity. For instance, *ku* mutants are immunodeficient and exhibit an

accelerated senescence (in correlation with the deregulation of telomere length), while LigaseIV deficiency leads to embryonic lethality in mice. In *Arabidopsis*, all characterized *nhej* mutants are viable but hypersensitive to various DNA damaging agents, except UV [5]. The *ku* mutants are hypersensitive to menadione (which causes oxidative damage), ionising radiations (X- and gamma-rays) and bleomycin (a radiomimetic), methylmethanesulfonate (MMS, an alkylating agent causing abasic sites and single-strand nicks) [4,5,7,8,9,10]. Hypersensitivity to MMS and gamma-irradiation has also been described for *ligIV* mutants [5,11]. Direct evidence for their involvement in NHEJ comes from plasmid rejoining assays. In protoplasts derived from *ku80* and *ku70* mutant plants, the religation efficiency of plasmids linearized by enzymes generating blunt or 5'overhang ends was significantly reduced [9,10].

The SSA and the HR pathways are homology-dependent processes for repairing DNA DSB. Both are initiated by the 5' to 3' resection of the broken DNA ends in order to uncover extensive single-stranded DNA (ssDNA) 3' overhangs, a critical intermediate in both SSA and HR. These 3' ssDNA tails are coated by the single-stranded DNA binding protein, RPA.

After DNA resection, the central step of SSA consists of the annealing between complementary single-stranded DNA sequences on either side of the DSB in a RAD52- and RAD59-dependent, but RAD51-independent, manner. Unpaired non-homologous 3' tails are then cleaved by the Rad1-Rad10 complex (XPF-ERCC1

in mammals), which is also involved in DNA excision repair, in order to complete the DSB repair with DNA synthesis from the newly cleaved ends and their final ligation. In *Arabidopsis*, mutants affected in *AtRAD1* (or *UVH1*) or *AtRAD10* (also called *AtERCC1*) activities have been identified as gamma- and UV-hypersensitive [12,13,14]. In contrast to XPF- or ERCC1-deficient mice, the corresponding single mutant plants are viable in the absence of exogenous DNA damaging agents, grow normally and are fertile. Using a plasmid recombination assay, it was shown that each gene was required for the removal of 3'-ended non-homologous DNA single-stranded tails from SSA intermediates, generated by annealing between direct repeats [15,16,17,18,19].

In contrast to NHEJ and SSA that are inherently error prone, HR is conservative, as it proceeds *via* the copy of the missing sequence from a homologous template. Moreover, HR is required during meiosis for correct chromosome segregation and the generation of genetic diversity. Meiotic recombination is initiated by the introduction of programmed DNA DSB catalyzed by the topoisomerase-like transesterase activity of dimeric Spo11. This leads to a covalent link between the catalytic tyrosine of a Spo11 monomer and the 5' DNA end on both sides of the DSB. In budding and fission yeast, removal of each Spo11 occurs by endonucleolytic cleavage several nucleotides downstream from the 5' end, catalyzed by the Mre11-Rad50-Xrs2 complex and Sae2. This releases a Spo11 monomer bound to an oligonucleotide, sometimes called a "spolligo" [20,21,22,23].

The repair process of HR in somatic and meiotic cells is initiated by extensive processing of DNA ends, uncovering 3' ssDNA stretches that become coated by RPA. This resection is essential for the establishment of a recombinase-DNA nucleofilament on the 3' single strand, which performs the homology search for a target DNA sequence to use as a template to copy, either the sister chromatid in somatic cells or a homologous chromosome in meiotic cells. Two recombinases can be loaded onto the ssDNA extension to mediate the strand displacement and homology search: the ubiquitous Rad51, the eukaryotic RecA homolog, and its homolog Dmc1 that has a specific role during meiosis. Once a homology is found, DSB repair is completed by DNA synthesis using the homologous sequence as a template and religation follows [24].

The displacement of RPA and its replacement by the recombinases rely on mediator proteins, such as the Rad51 paralogs, Rad52 and/or Brca2, which exist in most eukaryotes. In humans, *BRCA2* gene mutations are associated with hereditary breast cancer [25,26] and genome instability [27,28]. In mice, the knockout of *BRCA2* leads to early embryonic lethality associated with chromosomal rearrangements [29]. Structural and biochemical studies have shown the interaction between Rad51 and Brca2 [30,31,32]. Together with their co-localization in nuclear foci, after DNA damaging treatment of the cells, this definitively links Brca2 to homologous recombination [33].

Recently, the human Brca2 protein was purified [34,35,36]. It appears that one Brca2 molecule binds approximately six Rad51 monomers and that Brca2 stimulates the binding of Rad51 onto ssDNA even when it is covered by RPA. This interaction is mediated through the specific BRC domains which are present in all Brca2 proteins, but in varying numbers depending on species. For example, eight BRC domains are found in human Brca2 [31], whereas only one is present in Brh2 and Ce-BRC2, the Brca2 homologs of *Ustilago maydis* and *Caenorhabditis elegans* (*C. elegans*), respectively [37,38]. In *Arabidopsis*, two *AtBRCA2* genes have been identified: on chromosomes IV (*AtBRCA2(IV)*, also named *AtBRCA2a*) and V (*AtBRCA2(V)* or *AtBRCA2b*). They encode two proteins of 1511 (*AtBRCA2a*) and 1155 amino acids

(*AtBRCA2b*), which share 94.5% identity and contain four BRC motifs each. The two *Arabidopsis* genes are expressed in floral buds and the proteins they encode have been shown to interact with both Rad51 and Dmc1, the meiotic-specific recombinase [39,40]. Recently, the Brca2-Dmc1 interaction has been confirmed in humans [41]. These data thus linked Brca2 to meiotic recombination for the first time.

The understanding of Brca2 function has been considerably hampered by the early embryonic lethality associated to knocking out BRCA2 in mouse. Clear evidence for the meiotic role of Brca2 came from *A. thaliana* and *C. elegans* since the absence of the Brca2 function is viable and only leads to sterility due to meiotic defects in both models [38,39]. Indeed, RNAi-inactivation of both *Arabidopsis BRCA2* genes, specifically during meiosis, caused sterile plants resulting from an improper meiosis with chromosomal aberrations: absence of bivalent formation, chromosomal entangling, bridges and fragmentation. This phenotype was dependent on the formation of meiotic DNA double-strand breaks as it was alleviated in a *spo11* mutant [39]. We hypothesized that in *A. thaliana* the chromosomal abnormalities observed upon depletion of Brca2 at meiosis could be the result of an alternative repair of the meiotic DSB, in the absence of HR [39]. In *C. elegans*, Martin et al. (2005) showed that the RNAi depletion of *LIGIV* significantly reduced meiotic chromosome aggregation in *Cebrc-2* single mutants and could give rise to chromosomal fragmentation. These observations suggested that NHEJ could be partially responsible for the aberrant chromosome fusions in the absence of *CeBRC-2*.

In this study, the meiotic defects previously observed in Brca2-inactivated plants were confirmed in *brca2* double mutant plants containing a T-DNA insertion in each *AtBRCA2* gene. The potential role of alternative DNA repair pathways in the meiotic phenotype was tested by inactivating Brca2 in *nhej* and/or *ssa* mutant backgrounds. We demonstrate that neither NHEJ nor SSA were responsible for the observed cytological defects. Moreover, based on the hypothesis that covalent repair is responsible for the observed meiotic chromosomal defects in the absence of Brca2, we tested the role of a recently characterized plant-specific DNA ligase, AtLigase6. Since the abnormal meiotic figures were maintained in *lig6* plants inactivated for Brca2, the role of this DNA ligase during meiosis in the absence of HR was excluded.

## Results

### A *brca2* double mutant exhibits the same meiotic phenotype as Brca2-inactivated plants

In a previous study, *AtBRCA2a* and *AtBRCA2b* expression was inactivated during meiosis by RNAi using an inverted 510 pb-fragment of the *BRCA2* cDNA under the control of the meiotic-specific promoter of *DMC1* (*pDMC1*) [39]. In this work, single and double T-DNA insertion mutants for *AtBRCA2* were isolated and their phenotype compared to the RNAi-inactivated plants (named *pDMC1::RNAi/BRCA2*). First, *brca2* plants mutated in the *AtBRCA2* genes *via* either a T-DNA insertion located in the 10<sup>th</sup> intron of *AtBRCA2a* (in the Cter DNA binding domain) or an insertion in the 4<sup>th</sup> exon of *AtBRCA2b* (in the Nter domain of the protein, containing the BRC motifs) were isolated (Figure 1A and Figure 1B). *AtBRCA2* transcripts were analysed by RT-PCR, using primers flanking the insertion sites in wild-type and in *brca2* single mutant plants. Transcripts of the disrupted genes were not detected in the corresponding mutant lines, whereas transcripts of each *AtBRCA2* gene were amplified in wild-type plants. This strongly suggested that the two single *brca2* lines were null mutants (Figure 1C). Each single mutant showed normal development and

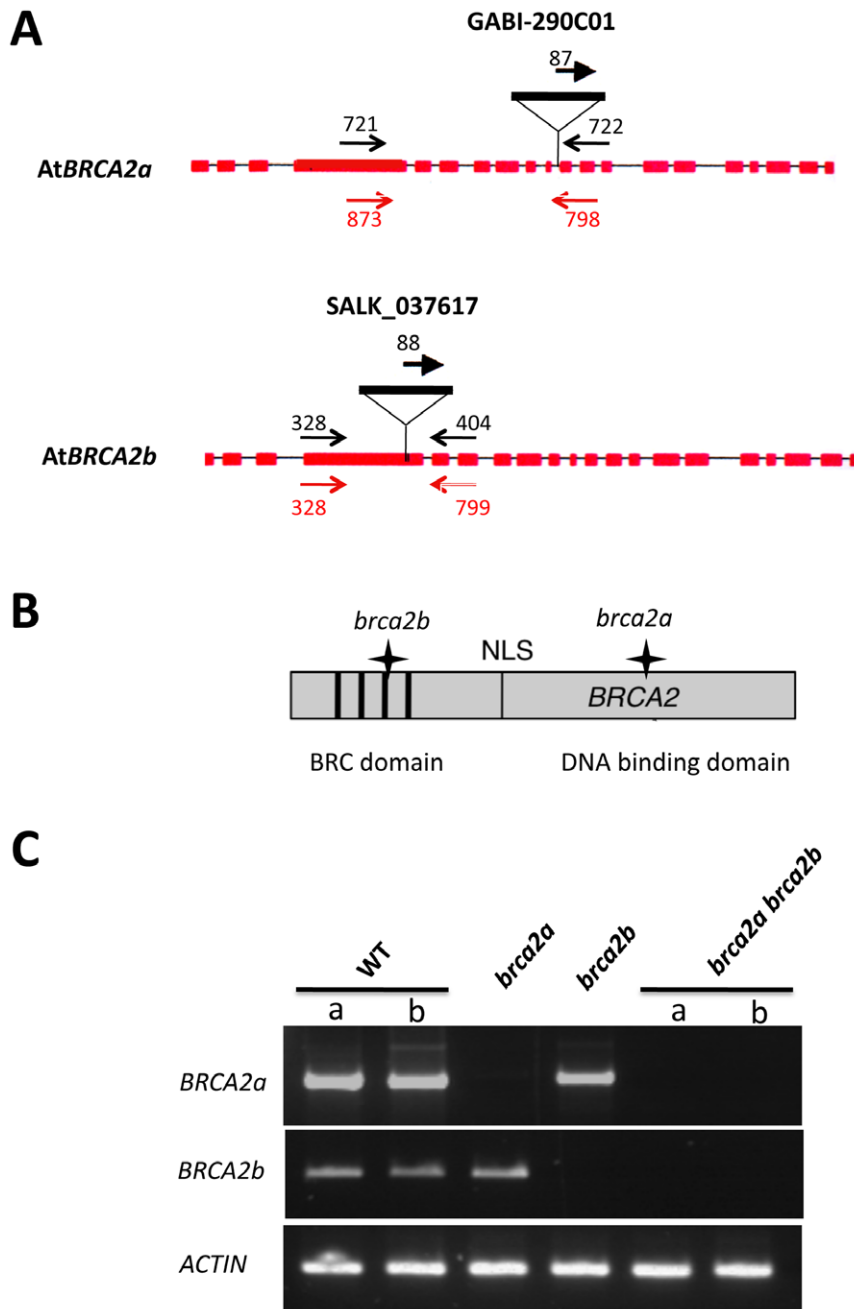


**Figure 1. The *brca2* single and double mutants.** (A) Position of the T-DNA insertions in *AtBRCA2a* and *AtBRCA2b*. The structure of the *AtBRCA2a* and *AtBRCA2b* genes is represented by shaded boxes (exons) and thin lines (introns). The T-DNA insertion position is indicated. Each primer pair used to identify the mutants by PCR are compiled on the diagram in black and primer pairs used for RT-PCR analyses are given in red; their localization is correct but not to scale. (B) Schematically represented Brca2 protein with the position of the BRC repeats and the NLS relative to the T-DNA insertions, as indicated by a star. For convenience, and because they share 94.5% of identity, a single Brca2 protein is represented. (C) RT-PCR analysis of *AtBRCA2* transcripts in the single and double *brca2* mutants. RNA was extracted from young floral buds of wild-type plants (2 different plants, a and b) as well as of *brca2a*, *brca2b* and *brca2a brca2b* (2 different plants, a and b) mutant plants and was then reverse-transcribed. Double-stranded cDNAs were then PCR-amplified using the primer pairs represented in red in Figure 1A. The constitutive *ACTIN* gene transcript was used as a control. doi:10.1371/journal.pone.0026696.g001

fertility. By crossing the single mutants, the double *brca2a brca2b* mutant was obtained. These latter plants showed no growth defect and behaved as the wild-type under normal greenhouse conditions. However, they were partially sterile producing very short and mostly empty siliques (Figure 2A). Moreover, the presence of meiotic defects was observed after DAPI staining of the chromosomes in the meiocytes. Indeed, all meiotic figures showed

chromosomal entangling without bivalent formation, bridges and fragmentation, leading to chromosomal missegregation (Figure 2B) as previously described for *pDMC1::RNAi/BRCA2* plants. A transgene containing a full length *AtBRCA2a* cDNA under the control of the promoter of the meiotic recombinase Dmc1 (*pDMC1::cDNA AtBRCA2a*) was introduced in 13 *brca2a brca2b* double mutant plants. 11 transformant plants presented a restored

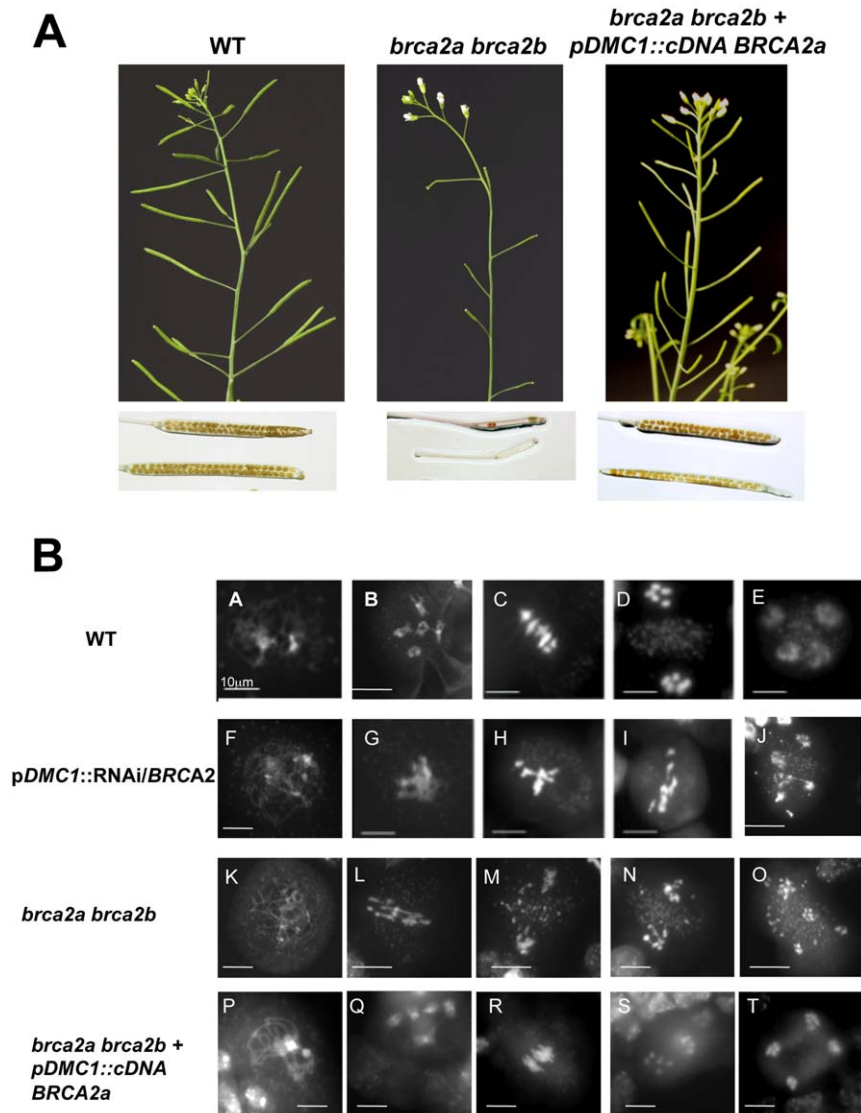


**Figure 2. Meiotic defects in *brca2a brca2b* mutant plants and in wild-type Brca2-inactivated plants. (A)** Wild-type and *brca2* double mutant plants exhibit no growth defect except for sterility. Chloralhydrate discolored siliques are full of seeds in wild-type plants in comparison with the discolored siliques of the *brca2* double mutant plants. **(B)** Observation of meicyotes by DAPI staining in Brca2-deficient plants, transformed or not with the full length cDNA of AtBRCA2a, and in *brca2a brca2b* homozygous double mutant plants. (A–E) Different stages of meiosis in the wild-type plants. Meiosis is normal. (A) Prophase I stage, (B) diakinesis, the five bivalents are attached by a chiasma, (C) metaphase I with five aligned bivalents, (D) anaphase I, bivalents segregate into two sets of five univalents, (E) anaphase II, with four groups that contain five chromosomes each after sister chromatid separation. (F–J) Different stages of meiosis in wild-type plants transformed with the *pDMC1::RNAi/BRCA2* construct. (F) Prophase I, (G) no normal diakinesis phase (H) metaphase I with condensed and entangled chromosomes, (I) anaphase I, with entangled and stretched chromosomes. (J) Anaphase II, with bridges extending between chromosomes. (K–O) Different stages of meiosis in *brca2* double mutant plants. (K) Prophase I, (L) anaphase I, entangled and stretched chromosomes. (M) Metaphase II with entangled chromosomes. (N) anaphase II, fragmented chromosomes. (O) telophase II with chromosome missegregation. (P–T) Different stages of meiosis in *brca2* double mutant plants, transformed with the *pDMC1::cDNA AtBRCA2a*. Meiosis is restored to normal. (P) Prophase I stage, (Q) diakinesis, (R) metaphase I, (S) anaphase I, (T) anaphase II. Bar 10  $\mu\text{m}$ . doi:10.1371/journal.pone.0026696.g002

phenotype: 9 were completely fertile as demonstrated by the observation of wild-type siliques content and normal meiosis (Figure 2) and 2 were partially fertile (as they presented some siliques that developed as sterile). Only 1 transformant was sterile with developmental defects. As a control, 11 *brca2a brca2b* double mutant plants were transformed with a transgene containing the *pDMC1::RNAi/0* construct, corresponding to the “empty vector” [39]: all of them were sterile (data not shown). These results reinforce the evidence for the role of AtBRCA2 at meiosis, previously uncovered by our RNAi strategy.

#### Characterization of *nhej* and *ssa* mutant plants by RT-PCR and under various genotoxic stress

In order to identify the molecular pathways involved in the aberrant cytological phenotype observed in the Brca2-deficient plants during meiosis, mutant plants deficient in either the NHEJ (*ku80<sup>-/-</sup>* and *ligIV<sup>-/-</sup>*) or the SSA (*erc1<sup>-/-</sup>*) pathways were characterized. Examining amplification of these transcripts specifically in meicyotes was not possible, as meicyotes would have to be specifically dissected which is technically difficult. However, as shown in Figure 3, all these three genes, and thus the

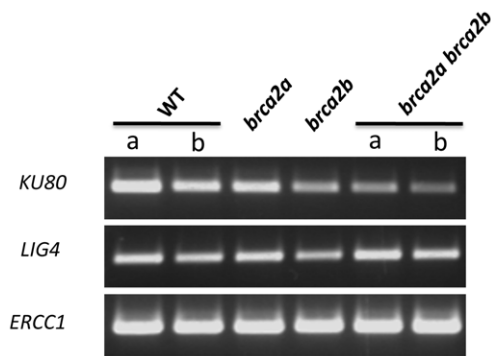


**Figure 3. RT-PCR analysis of genes involved in NHEJ and SSA in the single and double *brca2* mutants.** RNA was extracted from young floral buds and reverse-transcribed, as described in Figure 1C. Double-stranded cDNAs were PCR-amplified using primer pair 454/455 for *AtKU80* (see primer positions in Figure 4 and sequences in Table 1), 336/445 for *AtLIGIV* and 452/453 for *AtERCC1* (see Table 1 for sequences). The constitutive *ACTIN* gene transcript used as a control is presented in Figure 1C.  
doi:10.1371/journal.pone.0026696.g003

pathways they are involved in, were found expressed in young flower buds, where meiosis takes place, in single as well as in double *brca2* mutant plants. Two mutant lines have been previously described: SALK\_044027, where the T-DNA insertion is in exon 6 of the *AtLIGIV* gene [42,43] and SALK\_033397 which contains a T-DNA insertion in exon 3 of *AtERCC1* [16]. The absence of transcripts corresponding to the affected gene was confirmed for each mutant line by RT-PCR using primers flanking each T-DNA insertion (data not shown). The *ku* mutant line used in this study (SALK\_112921) had not been characterized to date. It contains a T-DNA in the 6<sup>th</sup> intron of the *AtKU80* gene (Figure 4A). RT-PCR analysis of the 5' and 3' regions flanking the T-DNA insertion revealed the presence of *AtKU80* transcripts in both wild-type and *ku80* mutant plants (Figure 4B). However, no transcripts could be detected in *ku80* mutant plants when primers flanking the T-DNA insertion were used, suggesting that splicing of the 6<sup>th</sup> intron did not occur in the *ku80* mutant. As the insertion site is positioned in the region encoding the domain involved in hetero-dimerization with Ku70, it is most likely that a putative protein, lacking this domain, would be non-functional. Thus, these *ku80* plants were considered as functional null mutants. The mutant plants, whatever the affected DNA repair pathway, exhibited no obvious developmental defects under normal growth conditions and were fertile, as previously described for *ercc1*, *ku80* and *ligIV Arabidopsis* mutants [9,13,16].

We believed that in the absence of HR during meiosis, the different DNA DSB repair pathways could compensate for each other. Thus, *nhej* mutant plants, *ku80* and *ligIV*, were crossed with *ssa* mutant plants, *ercc1*, and double *ku80 ercc1* and *ligIV ercc1* mutants affected in both pathways were isolated and genotyped. Both double mutants were viable, presented no obvious developmental defects under normal growth conditions and were fertile.

Sensitivity to various DNA damaging agents is a classical assay to characterize DNA repair mutant plants as most of them show no obvious somatic phenotype. To control that our mutants were indeed affected in DNA repair, their sensitivity to MMS, gamma-ray and UV irradiation was assayed. In comparison to wild-type plants, root growth was affected in the *nhej* plants as well as in the *ssa* plants in the presence of MMS or after gamma exposure. Indeed, the MMS hypersensitivity was visible at 50 ppm and gamma-ray hypersensitivity was observed at 100 grays for each

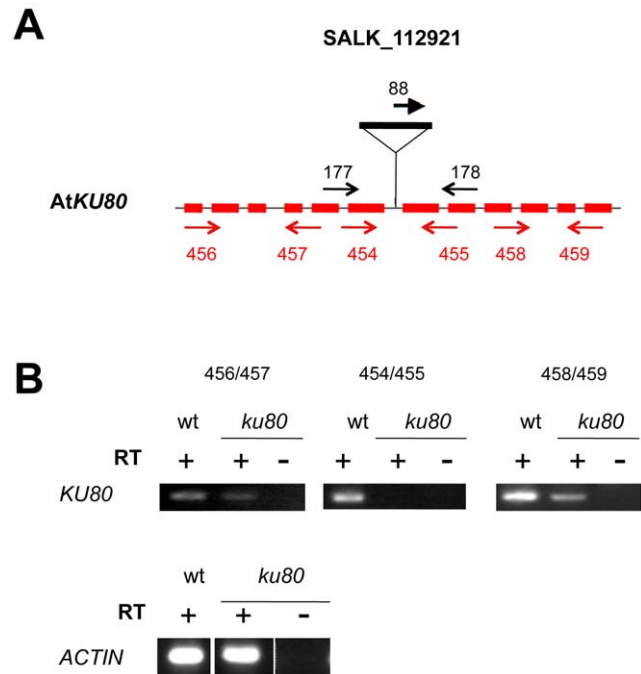


**Figure 4. T-DNA insertion and expression in *ku80* mutant.** (A) Position of the T-DNA insertion in *AtKU80*. The structure of the *AtKU80* gene is represented by shaded boxes (exons) and thin lines (introns). The T-DNA insertion position is indicated. Each primer pair used to characterize the mutant by PCR are indicated in black and primer pairs used for RT-PCR analyses are given in red; their localization is correct but not to scale. (B) RT-PCR analysis of *AtKU80* transcripts in *ku80* mutant plants. RNA, extracted from floral buds of wild-type or *ku80* mutant plants was reverse-transcribed. Double-stranded cDNAs were amplified by RT-PCR, performed with three different primer pairs: 5' or 3' to the T-DNA and flanking the T-DNA insertion. For primer positions, see above (Figure 4A). The constitutive *ACTIN* gene was used as a control.  
doi:10.1371/journal.pone.0026696.g004

single mutant line. However, MMS-induced retarded growth was more pronounced in *ercc1* than in *ku80* and *ligIV* plants (Figure 5A). MMS is a methylating agent, and due to the occurrence and clustering of modified bases, it can generate both SSB and DSB, which is reflected in the fact that *ercc1* mutants (deficient for both SSA and BER) appeared to be more sensitive to this genotoxic treatment. Reciprocally, *ercc1* plants were less sensitive to gamma irradiation when compared to *ku80* and *ligIV* (Figure 5B). Ionising radiations mainly give rise to clustered DNA damages (modified bases and abasic sites) that lead to DNA DSB. Such DNA strand breaks are mostly repaired by NHEJ as suggested by the higher hypersensitivity of *ku80* and *ligIV* mutants to gamma-rays. Finally, as expected, only the *ercc1* plants were hypersensitive to UV exposure (Figure 5C). All of these results confirmed that the different mutant *Arabidopsis* lines were affected in DNA DSB repair.

MMS and gamma-ray sensitivity of the double *nhej ssa* mutants were assessed in comparison to the single mutant plants (Figure 5). For each stress, we noted that the sensitivity of the double mutant was similar to that observed for the most affected single mutant: *ku80 ercc1* and *ligIV ercc1* appeared to be hypersensitive to MMS and UV as was the *ercc1* single mutant, whereas they showed a similar hypersensitivity to gamma-rays as the *nhej* single mutant. Therefore, no cumulative effect was observed.

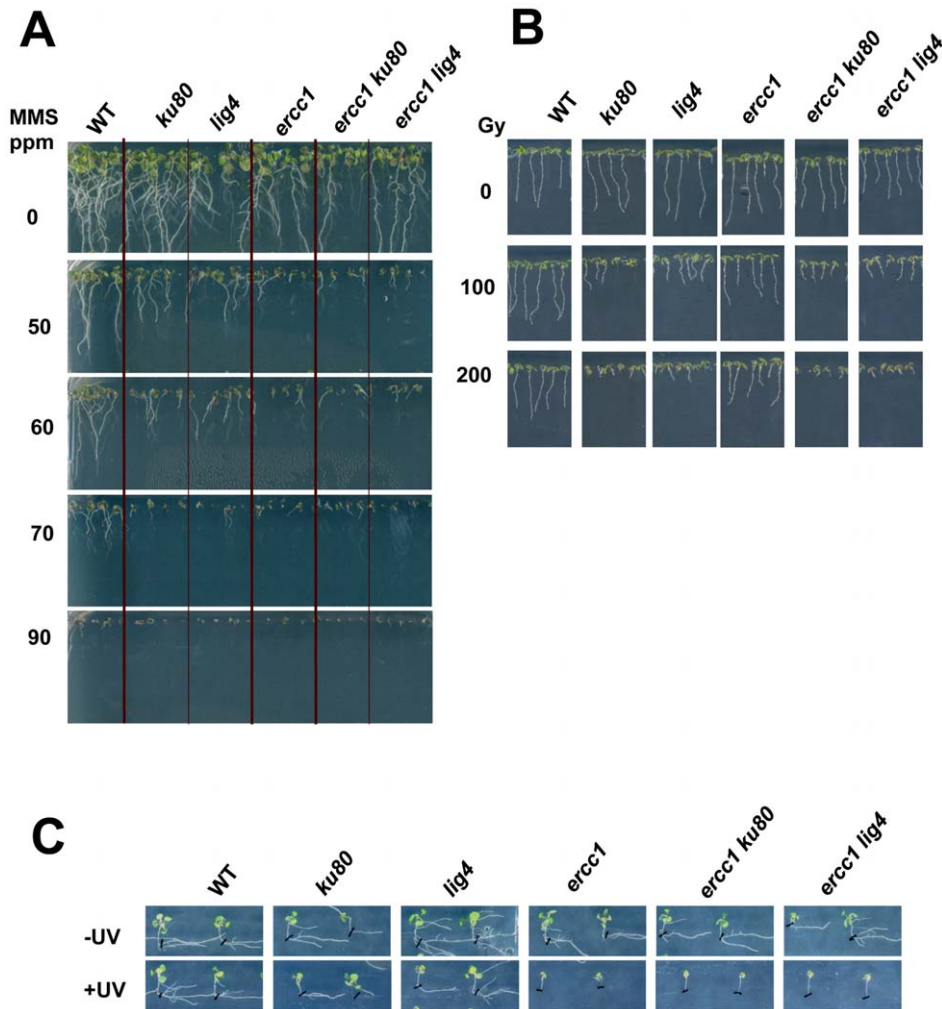


**Figure 5. Hypersensitivity to MMS, gamma-rays and UV irradiation of *nhej*, *ssa* and *nhej ssa* plants.** Before sowing, all seeds were surface-sterilized. **(A)** MMS hypersensitivity, 11 days post-germination. Seeds were sown on MS 0.5 agar 1% sucrose supplemented with MMS at various doses. **(B)** Gamma-irradiation hypersensitivity, 7 days post-irradiation. After 48 h at 4°C in darkness, seeds were exposed to various doses of gamma-rays : 0, 100 and 200 grays before being sown on MS 0.5 agar. **(C)** UV hypersensitivity, 10 days post-irradiation. Seeds were sown in MS 0.5 agar. After 4 days of growth, the plantlets were exposed to UV-C, left in the dark for 3 days to avoid photoreactivation, and then exposed to light. doi:10.1371/journal.pone.0026696.g005

### The *brca2* meiotic phenotype is maintained during meiosis in *nhej* and *ssa* backgrounds

The *Brca2* function was inactivated in the *nhej* and *ssa* mutant plants by transforming the mutant plants with the previously used *pDMC1::RNAi/BRCA2* construct. As a control, mutant plants were also transformed with a *pDMC1::RNAi/0* construct containing no insert [39]. No somatic phenotype was observed in any of the transformed plants containing the “empty” construct or the *pDMC1::RNAi/BRCA2* construct. When flowers emerged, all plants containing the control construct were fertile, whereas most of the mutant plants transformed with *pDMC1::RNAi/BRCA2* were partially sterile in the single *nhej* or *ssa* mutants (between 67 to 80%) as well as in the double *nhej ssa* mutants (between 60 to 78%), as previously observed for wild-type *pDMC1::RNAi/BRCA2* transformed plants.

The meiotic behaviour was examined after DAPI staining of the chromosomes in the meocytes of several independent transformed plants that were inactivated for the *Brca2* function: 175 meiotic figures from two *ku80*, 170 meioses from two *ligIV* and 34 meioses from two *ercc1* lines independently transformed with the

*pDMC1::RNAi/BRCA2* construct were observed. As a control, they were compared to the meioses of one *ku80*, one *ligIV* and one *ercc1* plant containing the *RNAi/0* construct. All of the observed control plant meiotic figures were normal in the single mutants affected for either NHEJ (*ku80*, *ligIV*) or SSA (*ercc1*), as well as in the *nhej ssa* double mutant (Supplementary Figure S1). On the other hand, meiosis was profoundly disturbed in meocytes of these same mutant lines transformed with the *pDMC1::RNAi/BRCA2* construct: chromosomal entangling without bivalent formation, fragmentation, and missegregation of chromosomes (Figure 6). Such observations have been previously reported in wild-type *pDMC1::RNAi/BRCA2* plants [39]. These observations suggested that, contrary to our hypothesis, in the absence of *Brca2* during meiosis, neither NHEJ nor SSA were responsible for an alternative meiotic DSB repair that would have been revealed because of the absence of HR [39]. The impact of the inactivation of both pathways in the absence of *Brca2* during meiosis was also examined. Meiotic figures from one *pDMC1::RNAi/BRCA2* transformant for *ercc1 ku80* (257 meiotic events, among them 80 were post-prophase) and two *pDMC1::RNAi/BRCA2* transformants for *ercc1 lig4* (115

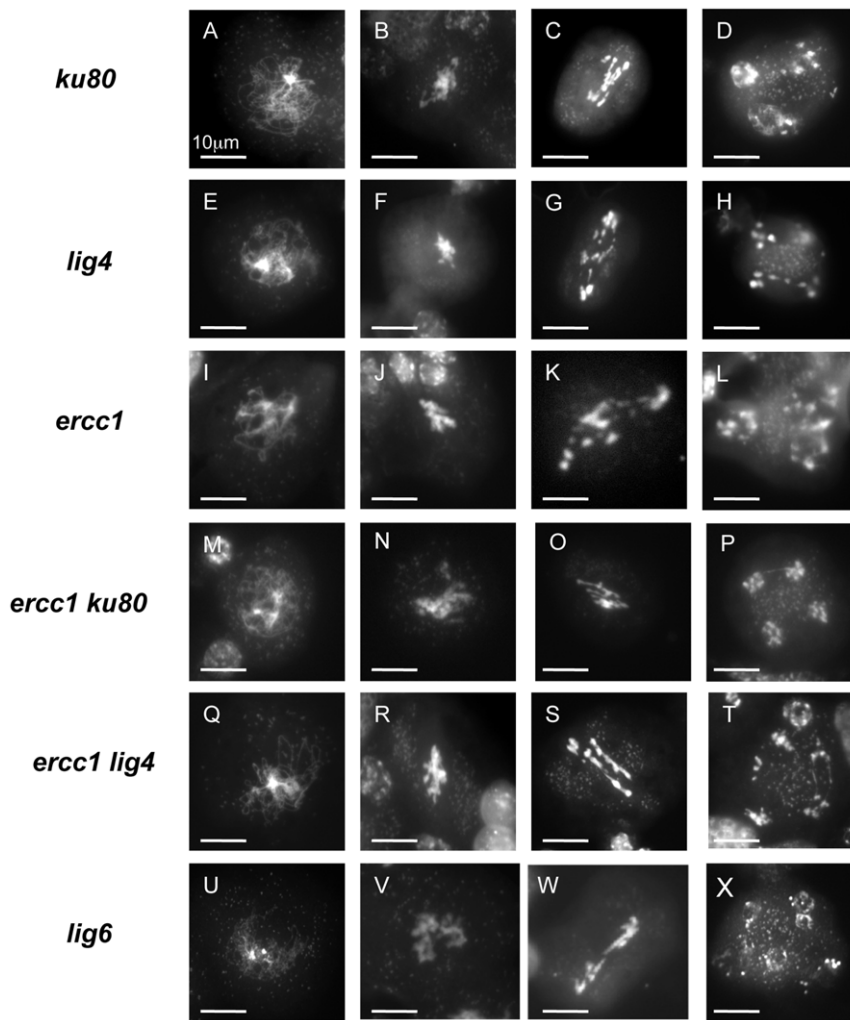


**Figure 6. Observation of meiotic cells by DAPI staining in *nhej*, *ssa*, *nhej ssa* and *lig6* mutant plants transformed with the pDMC1::RNAi/BRCA2 construct.** Different stages of meiosis were observed in plants transformed with pDMC1::RNAi/BRCA2 in *nhej* mutant plants, *ku80* (A–D) or *lig4* (E–H), and in *ssa* mutant plants, *ercc1* (I–L), in *nhej ssa* double mutant plants, *ercc1 ku80* (M–P) or *ercc1 lig4* (Q–T) and in *lig6* mutant plants (U–X). (A, E, I, M, Q, U) prophase I. (B, F, J, N, R, V) metaphase I. (C, G, K, O, S, W) anaphase I. (D, H, L, P, T, X) anaphase II. Bar 10 µm. doi:10.1371/journal.pone.0026696.g006

meiosis, including 63 post-prophase stages) were observed. In all double mutant plants transformed with pDMC1::RNAi/BRCA2, the *brca2* meiotic phenotype remained unaltered (Figure 6).

All of these results suggest that 1) the aberrant chromosomal figures observed in the absence of Brca2 during meiosis are not due to NHEJ or SSA and 2) the other major DNA DSB repair pathways, in the absence of HR, do not compensate for each other during meiosis.

### DNA Ligases in Arabidopsis

Our initial hypothesis was that the chromosomal bridges detected in the “failed” anaphases in the absence of Brca2 were due to covalent DNA links, probably between non-homologous chromosomes. Since our data exclude the role of NHEJ and SSA, all DNA ligases apart from LigaseIV (the NHEJ specific enzyme already studied in this work) could be potentially incriminated. The *Arabidopsis* genome contains three other sequences encoding DNA ligases: *AtLigase1* which is involved in replication and Base Excision Repair (BER), *AtLigase1a* which shares 71% identity with *AtLigase1* but for which no transcripts could be detected (our personal

data and transcriptome analyses: [http://csbdb.mpimp-golm.mpg.de/csbdb/dbxp/ath/ath\\_xpmsgq.html](http://csbdb.mpimp-golm.mpg.de/csbdb/dbxp/ath/ath_xpmsgq.html)), suggesting that it may be a pseudogene, and *AtLigase6*, a plant specific ligase that appears to be involved in seed longevity [44]. *AtLigase6* has a highly conserved DNA ligase catalytic domain and a beta-lactamase domain containing a beta-CASP motif found in Artemis and other proteins known to play a role in nucleic acid processing [45,46]. Since *lig1* mutant plants are embryonic lethal [47,48], we thus examined whether the plant specific *AtLigase6* could be involved in the meiotic phenotype of the Brca2-deficient plants.

Homozygous *lig6* plants containing a T-DNA insertion in exon 11 of the gene were obtained from the SALK collection (SALK\_065307) (Figure 7A). All plants grew normally, they were fertile and undertook normal meioses (data not shown). These observations are in agreement with what was previously observed in a different *lig6* insertional line (Waterworth et al, 2010) [44]. RT-PCR analyses detected transcripts on both sides of the T-DNA insertion but no transcripts could be found when primers flanking the T-DNA insertion were used (Figure 7B). As the T-DNA insertion is positioned in an exon, 42 bp from the codon of the catalytic lysine just upstream from the conserved motif II [49]



**Figure 7. T-DNA insertion and expression in *lig6* mutant. (A)** Position of the T-DNA insertion in *AtLIGASE 6*. The structure of the *AtLIGASE 6* gene is represented by shaded boxes (exons) and thin lines (introns). The T-DNA insertion position is indicated. Each primer pair used to identify the mutants by PCR are indicated in black while primer pairs used for RT-PCR analyses are given in red; their localization is correct but not to of scale. **(B)** RT-PCR analysis of *AtLIGASE 6* transcripts in *lig6*<sup>-/-</sup> mutant plants. RNA, extracted from floral buds of wild-type or *lig6* mutant plants was reverse-transcribed. Double-stranded cDNAs were amplified by RT-PCR, performed with three different primer pairs: 5' or 3' to the T-DNA and flanking the T-DNA. The position of each primer is given above (Figure 7A). The constitutive *ACTIN* gene was used as a control. doi:10.1371/journal.pone.0026696.g007

lying in the core domain, and more specifically around the nucleotide binding pocket responsible for the nucleotidyl transfer, the catalytic activity of a putatively expressed protein in this mutant is probably non-functional.

### DNA Ligase6 is not responsible for the *brca2* meiotic phenotype

Waterworth et al. (2010) observed a slight but significant growth hypersensitivity of *lig6* plants after a 100 Gy X-ray irradiation, leading them to suggest that *AtLigase6* could play a minor role in the repair of X-ray induced DNA damage. Transformation of our *lig6* mutant plants with *pDMC1::RNAi/BRCA2* was performed to inactivate the Brca2 function in *lig6* plants. 87% of the transformants (26/30) were partially sterile while *lig6* plants or *pDMC1::RNAi/0* transformed plants (six transformed plants, 57 meioses observed from two independent transformants) were normally fertile (Supplementary Figure S1). After DAPI staining of the chromosomes in the meocytes of seven *lig6* plants, independently transformed with the *pDMC1::RNAi/BRCA2* construct (426 meiotic figures, including 219 post-prophase events), the *brca2* meiotic phenotype was consistently observed (Figure 6), thus excluding a role of *AtLigase6* in this phenotype.

### Discussion

In *Arabidopsis*, RNAi-inactivation of Brca2 during meiosis gave rise to a sterility phenotype due to an aberrant meiosis characterized by an absence of bivalent formation, chromosomal

entangling, fragmentation and missegregation. Such defects were Spo11-dependant, therefore an alternative DNA repair process was proposed to be responsible for an aberrant repair of meiotic DSB in the absence of HR. In this study, we show that *brca2* double mutant plants exhibit a similar meiotic phenotype when compared to the *pDMC1::RNAi/BRCA2* transformed plants. Moreover, our data clearly exclude the role of NHEJ and SSA in the aberrant meiotic chromosomal figures of Brca2-deficient plants.

### Phenotypic characteristics of Brca2-deficient plants

In this study, double *brca2a brca2b* mutant plants were shown to have no obvious phenotype in terms of vegetative growth, contrary to the occasional fasciation described by Abe et al. (2009). This may be explained by the use of different ecotypes. However, the double *brca2* mutant displayed the same meiotic phenotype as previously described for *pDMC1::RNAi/BRCA2* transformed plants. Each single mutant was fertile, indicating the functional redundancy of the two *AtBRCA2* genes at meiosis [50,51]. This could not have been concluded from the *pDMC1::RNAi/BRCA2* transformed plants, as both *AtBRCA2* genes were silenced by the RNAi construct. Previously it was found that *pDMC1::RNAi/BRCA2* transformed plants produced a few seeds that could have arisen from a partial silencing of the *AtBRCA2* genes. However, this does not appear to be the reason since in the present study, a few seeds were also produced by the double mutant plants (Figure 2A). Preliminary experiments showed that the seeds germinated, producing *brca2* double mutant plants that developed

normally, although not fertile. This could mean that in the absence of Brca2, HR could be partially functional and give rise to some rare normal meiosis events that were not detected in our observations. Alternatively, the abnormal meiosis we observed may not be always detrimental to the chromosomes. It will be of interest to follow the *brca2* cumulative phenotypes from generation to generation, to check if their meiotic (and somatic) phenotypes become exacerbated.

### NHEJ and SSA do not compensate for HR deficiency during meiosis

Our analyses of the chromosomes in the meiocytes by DAPI staining in the double *brca2a brca2b* mutants revealed that the depletion of Brca2 during meiosis led to the absence of bivalent formation and to chromosome aggregates, thus confirming our previous study of plants transformed with the *pDMC1::RNAi/BRC42* construct. In anaphase I, aberrant bridges between chromosomes were systematically observed. We hypothesized that these defects were due to covalent repair of meiotic DSB. NHEJ was the main candidate pathway we believed responsible for these aberrant chromosomal figures. FISH experiments would not have proven that the chromosomes involved in these anaphase bridges were covalently linked, just that they were occasionally aberrantly “associated”. Thus, the Brca2 function was inactivated in NHEJ- but also in SSA-deficient plants. In contrast to *C. elegans*, a role of NHEJ in these meiotic defects can now be excluded, since these aberrant chromosome aggregates were still present in the meiocytes of plants defective in NHEJ [38]. A similar conclusion can be drawn in the case of the SSA-deficient plants. Furthermore, the additive disruption of both the NHEJ and SSA pathways did not modify the *brca2* meiotic phenotype. This demonstrates that, in contrast to somatic cells where deletions and translocations can occur in mutants defective in HR due to the error-prone repair of accidental DNA DSB *via* NHEJ or SSA, neither of these two major DNA DSB repair pathways can compensate for the absence of HR during meiosis in *Arabidopsis*. During meiosis, as the introduction of DNA DSB is programmed, inhibition of the NHEJ and SSA pathways must be very strong to prevent them to compete for or to replace HR. More generally, it is conceivable that the DNA repair processes that are initiated by programmed DNA DSB must be very carefully controlled. If neither NHEJ nor SSA are responsible for the meiotic defects of Brca2 deficient plants, we cannot exclude the role of alternative DNA DSB repair pathways, such as the backup end-joining pathway involving Xrcc1 [52]. Hence, further studies should be addressed to analyse meiosis in triple mutants, deficient for all three pathways, in Brca2-inactivated plants. However, recent data suggest that DNA DSB are still repaired in somatic cells of irradiated plants, defective for HR, SSA, NHEJ and backup end-joining, suggesting that other DNA DSB repair process probably remain to be discovered [53].

### Covalent repair or not ?

To better understand the molecular mechanisms responsible for the chromosomal bridges observed during meiotic anaphases in the absence of Brca2, we investigated the putative role of DNA ligases. Four potential DNA ligases have been identified in *Arabidopsis*: the essential *AtLIGASE1* involved in DNA replication and BER, *AtLIGASE1a*, the NHEJ-specific *AtLIGASEIV*, and the plant-specific *AtLIGASE6*. As *AtLIGASE1a* seems to be a pseudogene, it was excluded from our study. Our results show that the NHEJ specific DNA LigaseIV and the plant-specific Ligase6 were not involved in the meiotic chromosomal defects resulting from the absence of Brca2. Thus, a putative role of a plant DNA ligase activity remains an open question. It is difficult

to study the role of DNA Ligase1 as it is essential to DNA replication driving homozygous *lig1* mutant plants to be embryolethal [47,48]. In order to by-pass the lethality of the *lig1* mutant, Waterworth et al (2009) reduced the expression of *AtLIGASE1* using an RNAi construct that was set under the control of the ubiquitous CaMV35S promoter [47]. The partially inactivated plants exhibited precocious flowering but as their growth and development were strongly affected, it was difficult to describe them as clearly fertile. Hence, it would be interesting to undertake a meiosis-specific inhibition of *AtLIGASE1* expression using the *pDMC1* meiotic promoter, as previously carried out for Brca2. Otherwise, another possibility to consider is that the chromosomes are not covalently linked and that other proteins involved in chromatid cohesion and synapsis could help maintain the aberrant chromosome associations observed in the absence of Brca2.

## Materials and Methods

### Plant material and growth conditions

*Arabidopsis thaliana* Columbia ecotype were used in this study. Mutant lines were identified in the T-DNA express database of the Salk Institute Genomic Analysis Laboratory (<http://signal.salk.edu>). The insertional mutant affected in *AtERCC1* (line SALK\_033397) and in *AtLIGIV* (line SALK\_044027) have been described previously [16,42,43] as well as the *AtBRC42b* insertion line (SALK\_037617) [50]. The newly characterized mutant lines were GABI\_290C01 for *AtBRCA2a*, SALK\_112921 for *AtKU80* and SALK\_065307 for *AtLIGASE6*. Wild-type and mutant *Arabidopsis* plants were cultivated in a greenhouse at 23°C under long day conditions (16 h light, 8 h dark, humidity 75%).

### Isolation of genomic DNA and genotyping of the plants

Plants were genotyped by PCR performed on genomic DNA extracted from leaves of 2–3 week-old plants in Edwards’ buffer [54]. 1/50 of the extracted DNA was used as a template for PCR with two gene-specific primers and one primer specific for the left border of the T-DNA (Salk or Gabi-Kat, depending on the mutant lines) in separate reactions (see Table 1 and Figures 1, 4 and 7). The wild-type allele was amplified with oligonucleotides 721/722 for the *AtBRCA2a* locus, 328/404 for *AtBRC42b*, 177/178 for *AtKU80*, and 510/509 for *AtLIGASE6*. The mutant allele was detected using primer 88 (Lba1) for SALK T-DNA lines or 87 (08409) for Gabi-Kat T-DNA lines and primer 772 for the *AtBRCA2a* locus, 404 for *AtBRC42b*, 178 for *AtKU80*, or 509 for *AtLIGASE6*. PCR reactions were performed in a 20 µl final volume, with 0.2 mM of dNTPs, 5 mM MgCl<sub>2</sub>, 1 µM of each primer, 1U of Taq DNA polymerase (Invitrogen<sup>TM</sup>). They were incubated in a 2720 Thermocycler (Applied Biosystem) at 94°C for 2 min, followed by 35 cycles at 94°C for 30 s, 50°C for 30 s and 72°C for 1 min, except for the PCR on the *AtBRCA2* genes where the annealing step was performed at 52°C for 30 s. The PCR samples were then visualized after migration on 0.7% agarose gels in the presence of ethidium bromide.

### RNA isolation and RT-PCR analyses

Total RNA was extracted from leaves or floral buds of 2–3 week-old individual plants with the NucleoSpin<sup>®</sup> RNA Plant (Macherey-Nagel) according to the manufacturers’ specifications. 2 µg of total RNA was used as a template for reverse-transcription with the RT ImProm II<sup>TM</sup> (Promega) and oligod(T) as a primer. 1/20 of the RT reactions were used as a template for PCR in a total volume of 50 µl. The quality of the RT reaction was controlled by examining actin expression by PCR using

**Table 1.** Sequence and use of primers in this study.

Name	Gene	DNA sequence (5'-3')	Use
87	Gabi T-DNA o8409	ATATTGACCATCATACTCATTGC	genotyping
88	Salk T-DNA LBa1	TGGTTCACGTAGTGGGCCATCG	genotyping
721	<i>AtBRCA2a</i> (At4g00020/10)	GATTGTGCTCTGAATGCTAC	genotyping
722	<i>AtBRCA2a</i> (At4g00020/10)	CAATTTCTTTACCTTGAGGA	genotyping
873	<i>AtBRCA2a</i> (At4g00020/10)	ATGAGACCGATTGTGCTCTGAATGC	RT-PCR
798	<i>AtBRCA2a</i> (At4g00020/10)	CCAATTTCTTTACAGAAGCCTAGTCG	RT-PCR
328	<i>AtBRCA2b</i> (At5g01630)	GCTCTGAATATCAGTAAACCTGCT	genotyping and RT-PCR
404	<i>AtBRCA2b</i> (At5g01630)	TGTATCACACGATACAACAGACA	genotyping
799	<i>AtBRCA2b</i> (At5g01630)	TACAACAGACAAACCACTTGAAGCTTGCT	RT-PCR
177	<i>AtKU80</i> ((At1g48050)	TGCTTTTGTCTGTTGTGCAG	genotyping
178	<i>AtKU80</i> ((At1g48050)	GCAGAAGGTGCAAGGTCAAG	genotyping
456	<i>AtKU80</i> ((At1g48050)	ATGGCACGAAATCGGGAGGGTTTG	RT-PCR
457	<i>AtKU80</i> ((At1g48050)	ACGATCAAGAAAGTCTCCAGCTAC	RT-PCR
454	<i>AtKU80</i> ((At1g48050)	GAAGATTAAGGTGTGGGTTTATAAG	RT-PCR
455	<i>AtKU80</i> ((At1g48050)	GTAAAACGAATCAGGAGTATCATCTC	RT-PCR
458	<i>AtKU80</i> ((At1g48050)	CAAGGAGAATCCAAGTTGAAGAAGG	RT-PCR
459	<i>AtKU80</i> ((At1g48050)	CGTCTACTATACACTGTCCGCTG	RT-PCR
510	<i>AtLIGASE6</i> (At1g66730)	TCATTGCAGAATTGCTAAGGG	genotyping
509	<i>AtLIGASE6</i> (At1g66730)	GAAGACGCAGACTTCAACCTG	genotyping
637	<i>AtLIGASE6</i> (At1g66730)	AGAGCACGCTTGTGGAGGG	RT-PCR
638	<i>AtLIGASE6</i> (At1g66730)	TAAATTACGGGCCAATGTCTAACAAG	RT-PCR
686	<i>AtLIGASE6</i> (At1g66730)	GAGGGTGTCTGCTGCTAGTGTGAGGCTTACAA	RT-PCR
640	<i>AtLIGASE6</i> (At1g66730)	AAGAGCCAACAGCTGTCTCCA	RT-PCR
641	<i>AtLIGASE6</i> (At1g66730)	TTCATGGCTCAAGTTAAGCGAGAT	RT-PCR
642	<i>AtLIGASE6</i> (At1g66730)	GTTTGAGCATGAAACATCTCTGCGA	RT-PCR
Act-464	<i>AtACT2</i> (At3g18780)	TGAGACCTTTAACTCTCCCG	RT-PCR
Act-465	<i>AtACT2</i> (At3g18780)	GATGGCATGAGGAAGAGAGA	RT-PCR
336	<i>AtLIGIV</i> (At5g57160)	TTGCTGCTGAGGTATTGCAACGTAGAC	RT-PCR
445	<i>AtLIGIV</i> (At5g57160)	CCATCAAGGATACACTGTCCACCAAT	RT-PCR
452	<i>AtERCC1</i> (At3g05210)	CCCACAGTTCAAGCCAACGCATC	RT-PCR
453	<i>AtERCC1</i> (At3g05210)	ACATTCTGTCATGCTCCAGGCAC	RT-PCR

See figures 1, 4 and 7 for the relative position of the primers.  
doi:10.1371/journal.pone.0026696.t001

primers act-464 and act-465. For *AtBRCA2a* and *AtBRCA2b* cDNAs, specific primers flanking the T-DNA insertion were designed: 873/798 and 328/799 respectively (see Table 1 and Figure 1). For *AtKU80*, specific primers were designed 5' to the insertion (456/457), flanking the T-DNA insertion (454/455) and 3' to the T-DNA (458/459) (see Table 1 and Figure 4). For *AtLIGIV* and *AtERCC1* cDNAs, specific oligonucleotides were designed flanking their respective T-DNA insertion site: the 336/445 pair for *AtLIGIV* and the 452/453 pair for *AtERCC1* (see Table 1 for sequences). For *AtLIGASE6*, specific primers were designed 5' to the insertion (637/638), flanking the T-DNA insertion (686/640) and 3' to the T-DNA (641/642) (see Table 1 and Figure 7). The PCR was as follows: 94°C for 3 min, followed by 35 cycles at 94°C for 30 s, 50°C or 52°C for 30 s and 72°C for 1 min, except for the *ACTIN* gene (see Table 1 for sequences of the ACT2 primers) where the elongation step was performed at 58°C for 30 s. 20 µl of the RT-PCR reaction were then loaded onto a 3% agarose gel (NuSieve) in the presence of ethidium bromide for visualization.

#### pDMC1:: cDNA *AtBRCA2a* construct

The full length cDNA of *AtBRCA2a* was previously cloned in pUC18 as described in [39]. It was subsequently subcloned first into pKannibal [55] and then into the *XhoI-SpeI*-restricted pPF408 to be set under the pDMC1 promoter control [39].

#### In vitro assays for sensitivity to MMS, gamma-rays and UV

Seeds were surface-sterilized with a solution containing 50% bleach diluted in EtOH. Sterilized seeds were sown on MS 0.5 agar media (Kalys) containing 1% sucrose and supplemented with 0, 50, 60, 70, 80 or 90 ppm of MMS and then set at 4°C in the dark for 48 h to synchronize germination, before being placed vertically in the growth chamber for 14 days to allow the roots to grow along the agar surface. For irradiation experiments, sterilized seeds stored at 4°C in the dark were exposed to 0, 100 or 200 Grays from a <sup>137</sup>Cs source at a dose rate of approximately 50 gy.min<sup>-1</sup> (IBL-637 (CIS-BioInternational), Institut Curie, Orsay). After irradiation, they were sown on MS 0.5 agar media and set vertically in a growth chamber. After 11 days, root

growth was observed. For UV experiments, sterilized seeds were sown on MS 0.5 agar and after 4 days of vertical growth, the plantlets were exposed to  $540 \text{ J.m}^{-2}$  of UV-C (254 nm). The plates were then 90 degrees rotated, set in the dark for 3 days to avoid photoreactivation and then exposed 3 days to light to observe the recovery of main root growth of each seedling during two weeks.

### Plant crosses

Since all single mutants used in this study were fertile, double mutants were obtained by crossing two homozygous mutants affected in the gene of interest. Double mutants were identified by PCR of the F2 population obtained by self-fertilisation of F1 plants heterozygous for both genes.

### Transformation of plants with RNAi constructs

The RNAi constructs aimed at silencing both *BRCA2* genes and the control without any insert were previously described in [39]. Plant transformations were carried out by floral dip as described previously [56]. T1 transformants were selected on sand supplemented with Basta® and transferred to soil pots. Approximately one to two weeks after, the selected transformed plants were sprayed with Basta® (4% ammonium glufosinate) for a second control of their resistance.

### DAPI staining and cytology

The flower buds or the siliques were fixed in a solution of absolute ethanol and acetic acid (3/1 v/v) at room temperature. Chromosome spreads were prepared as in [57]. Photographs were captured using a Photometrics CoolsNAP EZ camera driven by Metavue 7.0 r4 software.

Fixed siliques were placed in ethanol 70% during 2 h, and then in a chloralhydrate solution (8 g/3 ml glycerol 66%) during a night in the dark. Images were captured on a Zeiss stereomicroscope Stemi SV1 with a SONY camera driven by Zeiss Axiovision Software.

### References

- Daley JM, Palmos PL, Wu D, Wilson TE (2005) Nonhomologous end joining in yeast. *Annu Rev Genet* 39: 431–451.
- Lieber MR (2010) The mechanism of double-strand DNA break repair by the nonhomologous DNA end-joining pathway. *Annu Rev Biochem* 79: 181–211.
- Tamura K, Adachi Y, Chiba K, Oguchi K, Takahashi H (2002) Identification of Ku70 and Ku80 homologues in *Arabidopsis thaliana*: evidence for a role in the repair of DNA double-strand breaks. *Plant J* 29: 771–781.
- Riha K, Watson JM, Parkey J, Shippen DE (2002) Telomere length deregulation and enhanced sensitivity to genotoxic stress in *Arabidopsis* mutants deficient in Ku70. *Embo J* 21: 2819–2826.
- Friesner J, Britt AB (2003) Ku80- and DNA ligase IV-deficient plants are sensitive to ionizing radiation and defective in T-DNA integration. *Plant J* 34: 427–440.
- West CE, Waterworth WM, Jiang Q, Bray CM (2000) *Arabidopsis* DNA ligase IV is induced by gamma-irradiation and interacts with an *Arabidopsis* homologue of the double strand break repair protein XRCC4. *Plant J* 24: 67–78.
- West CE, Waterworth WM, Story GW, Sunderland PA, Jiang Q, et al. (2002) Disruption of the *Arabidopsis* AtKu80 gene demonstrates an essential role for AtKu80 protein in efficient repair of DNA double-strand breaks in vivo. *Plant J* 31: 517–528.
- Bundock P, van Attikum H, Hooykaas P (2002) Increased telomere length and hypersensitivity to DNA damaging agents in an *Arabidopsis* KU70 mutant. *Nucleic Acids Res* 30: 3395–3400.
- Gallego ME, Bleuyard JY, Daoudal-Cotterell S, Jallut N, White CI (2003) Ku80 plays a role in non-homologous recombination but is not required for T-DNA integration in *Arabidopsis*. *Plant J* 35: 557–565.
- Wang YK, Chang WC, Liu PF, Hsiao MK, Lin CT, et al. (2010) Ovate family protein 1 as a plant Ku70 interacting protein involving in DNA double-strand break repair. *Plant Mol Biol* 74: 453–466.
- van Attikum H, Bundock P, Overmeer RM, Lee LY, Gelvin SB, et al. (2003) The *Arabidopsis* AtLIG4 gene is required for the repair of DNA damage, but not for the integration of *Agrobacterium* T-DNA. *Nucleic Acids Res* 31: 4247–4255.
- Preuss SB, Jiang CZ, Baik HK, Kado CI, Britt AB (1999) Radiation-sensitive *Arabidopsis* mutants are proficient for T-DNA transformation. *Mol Gen Genet* 261: 623–626.
- Hefner E, Preuss SB, Britt AB (2003) *Arabidopsis* mutants sensitive to gamma radiation include the homologue of the human repair gene ERCC1. *J Exp Bot* 54: 669–680.
- Fidantsef AL, Mitchell DL, Britt AB (2000) The *Arabidopsis* UVH1 gene is a homolog of the yeast repair endonuclease RAD1. *Plant Physiol* 124: 579–586.
- Dubest S, Gallego ME, White CI (2002) Role of the AtRad1p endonuclease in homologous recombination in plants. *EMBO Rep* 3: 1049–1054.
- Dubest S, Gallego ME, White CI (2004) Roles of the AtErcc1 protein in recombination. *Plant J* 39: 334–342.
- McWhir J, Selfridge J, Harrison DJ, Squires S, Melton DW (1993) Mice with DNA repair gene (ERCC-1) deficiency have elevated levels of p53, liver nuclear abnormalities and die before weaning. *Nat Genet* 5: 217–224.
- Weeda G, Donker I, de Wit J, Morreau H, Janssens R, et al. (1997) Disruption of mouse ERCC1 results in a novel repair syndrome with growth failure, nuclear abnormalities and senescence. *Curr Biol* 7: 427–439.
- Tian M, Shinkura R, Shinkura N, Alt FW (2004) Growth retardation, early death, and DNA repair defects in mice deficient for the nucleotide excision repair enzyme XPF. *Mol Cell Biol* 24: 1200–1205.
- Neale MJ, Pan J, Keeney S (2005) Endonucleolytic processing of covalent protein-linked DNA double-strand breaks. *Nature* 436: 1053–1057.
- Hartsuiker E, Mizuno K, Molnar M, Kohli J, Ohta K, et al. (2009) Ctp1CtIP and Rad32Mre11 nuclease activity are required for Rec12Spo11 removal, but Rec12Spo11 removal is dispensable for other MRN-dependent meiotic functions. *Mol Cell Biol* 29: 1671–1681.
- Milman N, Higuchi E, Smith GR (2009) Meiotic DNA double-strand break repair requires two nucleases, MRN and Ctp1, to produce a single size class of Rec12 (Spo11)-oligonucleotide complexes. *Mol Cell Biol* 29: 5998–6005.
- Cole F, Keeney S, Jasin M (2010) Evolutionary conservation of meiotic DSB proteins: more than just Spo11. *Genes Dev* 24: 1201–1207.

All images were further processed with Adobe Photoshop CS2.

### Supporting Information

**Figure S1 Observation of meiocytes by DAPI staining in *nhej*, *ssa*, *nhej ssa* and *lig6* mutant plants transformed with the RNAi/0 control construct.** Normal meiotic progression in plants transformed with pDMC1::RNAi/0 in *nhej* mutant plants, *ku80* (A–B) and *lig4* (C–D), in the *ssa* mutant *ercc1* (E–F), in double *nhej ssa* mutants *ku80 ercc1* (G–H) and *lig4 ercc1* (I–J), and in *lig6* mutant plants (K–L). Bivalents were correctly associated during the first meiotic phase (diakinesis (A–E–G–K) and metaphase I (C, I). Segregation of homologous chromosomes and during the second division, sister chromatid separation occurred normally without chromosomal bridges or fragmentation (metaphase II or early anaphase II (L), anaphase II (B–D–H–J) plants, and telophase II (F)). Bar 10  $\mu\text{m}$ . (TIF)

### Acknowledgments

We are grateful to Thierry Lagrange and Sylvie Lamy for kindly providing the T-DNA insertion line disrupted in *AtBRCA2a* (GK\_290C01) and PCR genotyping conditions, Sophie Blanchet for the *ACTIN* primers (ACT2) and PCR conditions for RT-PCR. The service of Dr V. Favaudon at Institut Curie (Orsay) is thanked for access to the  $^{137}\text{Cs}$  irradiator. We also thank Michael Hodges and Mireille Bétermier for critical reading of the manuscript, and Guillaume Blayo and Patricia Racine for their technical contribution.

### Author Contributions

Conceived and designed the experiments: AG MPD MD. Performed the experiments: MD SM. Analyzed the data: AG MPD MD. Contributed reagents/materials/analysis tools: MD SM. Wrote the paper: AG MPD MD.

24. San Filippo J, Sung P, Klein H (2008) Mechanism of eukaryotic homologous recombination. *Annu Rev Biochem* 77: 229–257.
25. Wooster R, Bignell G, Lancaster J, Swift S, Seal S, et al. (1995) Identification of the breast cancer susceptibility gene BRCA2. *Nature* 378: 789–792.
26. Scully R, Livingston DM (2000) In search of the tumour-suppressor functions of BRCA1 and BRCA2. *Nature* 408: 429–432.
27. West SC (2003) Molecular views of recombination proteins and their control. *Nat Rev Mol Cell Biol* 4: 435–445.
28. Jasin M (2002) Homologous repair of DNA damage and tumorigenesis: the BRCA connection. *Oncogene* 21: 8981–8993.
29. Yu VP, Koehler M, Steinlein C, Schmid M, Hanakahi LA, et al. (2000) Gross chromosomal rearrangements and genetic exchange between nonhomologous chromosomes following BRCA2 inactivation. *Genes Dev* 14: 1400–1406.
30. Sharan SK, Morimatsu M, Albrecht U, Lim DS, Regel E, et al. (1997) Embryonic lethality and radiation hypersensitivity mediated by Rad51 in mice lacking Brca2. *Nature* 386: 804–810.
31. Wong AK, Pero R, Ormonde PA, Tavtigian SV, Bartel PL (1997) RAD51 interacts with the evolutionarily conserved BRC motifs in the human breast cancer susceptibility gene brca2. *J Biol Chem* 272: 31941–31944.
32. Pellegrini L, Yu DS, Lo T, Anand S, Lee M, et al. (2002) Insights into DNA recombination from the structure of a RAD51-BRCA2 complex. *Nature* 420: 287–293.
33. Tarsounas M, Davies AA, West SC (2004) RAD51 localization and activation following DNA damage. *Philos Trans R Soc Lond B Biol Sci* 359: 87–93.
34. Jensen RB, Carreira A, Kowalczykowski SC (2010) Purified human BRCA2 stimulates RAD51-mediated recombination. *Nature* 467: 678–683.
35. Thorslund T, McIlwraith MJ, Compton SA, Lekomtsev S, Petronczki M, et al. (2010) The breast cancer tumor suppressor BRCA2 promotes the specific targeting of RAD51 to single-stranded DNA. *Nat Struct Mol Biol* 17: 1263–1265.
36. Liu J, Doty T, Gibson B, Heyer WD (2010) Human BRCA2 protein promotes RAD51 filament formation on RPA-covered single-stranded DNA. *Nat Struct Mol Biol* 17: 1260–1262.
37. Kojic M, Kostrub CF, Buchman AR, Holloman WK (2002) BRCA2 homolog required for proficiency in DNA repair, recombination, and genome stability in *Ustilago maydis*. *Mol Cell* 10: 683–691.
38. Martin JS, Winkelmann N, Petalcorin MI, McIlwraith MJ, Boulton SJ (2005) RAD-51-dependent and -independent roles of a *Caenorhabditis elegans* BRCA2-related protein during DNA double-strand break repair. *Mol Cell Biol* 25: 3127–3139.
39. Siaud N, Dray E, Gy I, Gerard E, Takvorian N, et al. (2004) Brca2 is involved in meiosis in *Arabidopsis thaliana* as suggested by its interaction with Dmc1. *Embo J* 23: 1392–1401.
40. Dray E, Siaud N, Dubois E, Doutriaux MP (2006) Interaction between *Arabidopsis* Brca2 and its partners Rad51, Dmc1, and Dss1. *Plant Physiol* 140: 1059–1069.
41. Thorslund T, Esashi F, West SC (2007) Interactions between human BRCA2 protein and the meiosis-specific recombinase DMC1. *Embo J* 26: 2915–2922.
42. Heacock ML, Idol RA, Friesner JD, Britt AB, Shippen DE (2007) Telomere dynamics and fusion of critically shortened telomeres in plants lacking DNA ligase IV. *Nucleic Acids Res* 35: 6490–6500.
43. Tanaka S, Ishii C, Hatakeyama S, Inoue H (2010) High efficient gene targeting on the AGAMOUS gene in an *Arabidopsis* AtLIG4 mutant. *Biochem Biophys Res Commun* 396: 289–293.
44. Waterworth WM, Masnavi G, Bhardwaj RM, Jiang Q, Bray CM, et al. (2010) A plant DNA ligase is an important determinant of seed longevity. *Plant J* 63: 848–860.
45. Callebaut I, Moshous D, Mormon JP, de Villartay JP (2002) Metallo-beta-lactamase fold within nucleic acids processing enzymes: the beta-CASP family. *Nucleic Acids Res* 30: 3592–3601.
46. Bonatto D, Revers LF, Brendel M, Henriques JA (2005) The eukaryotic Pso2/Snm1/Artemis proteins and their function as genomic and cellular caretakers. *Braz J Med Biol Res* 38: 321–334.
47. Waterworth WM, Kozak J, Provost CM, Bray CM, Angelis KJ, et al. (2009) DNA ligase I deficient plants display severe growth defects and delayed repair of both DNA single and double strand breaks. *BMC Plant Biol* 9: 79.
48. Andreuzza S, Li J, Guitton AE, Faure JE, Casanova S, et al. (2010) DNA LIGASE I exerts a maternal effect on seed development in *Arabidopsis thaliana*. *Development* 137: 73–81.
49. Timson DJ, Singleton MR, Wigley DB (2000) DNA ligases in the repair and replication of DNA. *Mutat Res* 460: 301–318.
50. Wang S, Durrant WE, Song J, Spivey NW, Dong X (2010) *Arabidopsis* BRCA2 and RAD51 proteins are specifically involved in defense gene transcription during plant immune responses. *Proc Natl Acad Sci U S A* 107: 22716–22721.
51. Abe K, Osakabe K, Ishikawa Y, Tagiri A, Yamanouchi H, et al. (2009) Inefficient double-strand DNA break repair is associated with increased fasciation in *Arabidopsis* BRCA2 mutants. *J Exp Bot* 60: 2751–2761.
52. Charbonnel C, Gallego ME, White CI (2010) Xrcc1-dependent and Ku-dependent DNA double-strand break repair kinetics in *Arabidopsis* plants. *Plant J* 64: 280–290.
53. Charbonnel C, Allain E, Gallego ME, White CI (2011) Kinetic analysis of DNA double-strand break repair pathways in *Arabidopsis*. *DNA Repair (Amst)* in press.
54. Edwards K, Johnstone C, Thompson C (1991) A simple and rapid method for the preparation of plant genomic DNA for PCR analysis. *Nucleic Acids Res* 19: 1349.
55. Helliwell C, Waterhouse P (2003) Constructs and methods for high-throughput gene silencing in plants. *Methods* 30: 289–295.
56. Clough SJ, Bent AF (1998) Floral dip: a simplified method for *Agrobacterium*-mediated transformation of *Arabidopsis thaliana*. *Plant J* 16: 735–743.
57. Couteau F, Belzile F, Horlow C, Grandjean O, Vezon D, et al. (1999) Random chromosome segregation without meiotic arrest in both male and female meicytes of a dmc1 mutant of *Arabidopsis*. *Plant Cell* 11: 1623–1634.